Manuscript submitted April 28, 1995; revised manuscript received Oct. 5, 1995.

Sophia University assisted in meeting the publication costs of this article.

REFERENCES

1. R. D. Westbrook, R. F. Wood, and G. E. Jellison, Jr., *Appl. Phys. Lett.*, **50**, 469 (1987).
2. A. Yoshida and K. Setsune, *IEEE Electron Devices Lett.*, **EDL-9**, 90 (1988).
3. A. Yoshida, M. Kitagawa, K. Setsune, and T. Hirao, *J. J. Appl. Phys.*, **27**, L1355 (1988).
4. M. Kitagawa, N. Matsuo, G. Fuse, H. Iwasaki, A. Yoshida, and T. Hirao, *ibid.*, **27**, L2139 (1988).
5. G. Kawachi, T. Aoyama, K. Miyata, Y. Ohno, A. Mimura, N. Konishi, and Y. Mochizuki, *This Journal*, **137**, 3522 (1990).
6. G. Kawachi, T. Aoyama, T. Suzuki, A. Mimura, Y. Ohno, N. Konishi, Y. Mochizuki, and K. Miyata, *Jpn. J. Appl. Phys.*, **29**, L2370 (1990).
7. K. Masumo, M. Kunigita, S. Takafuji, N. Nakamura, A. Iwasaki, and M. Yuki, *ibid.*, **29**, L2377 (1990).
8. A. Mimura, G. Kawachi, T. Aoyama, T. Suzuki, Y. Nagae, N. Konishi, and Y. Mochizuki, *IEEE Trans. Electron Devices*, **ED-40**, 523 (1993).
9. G. Kawachi, T. Aoyama, A. Mimura, and N. Konishi, *Jpn. J. Appl. Phys.*, **33**, 2092 (1994).
10. B. Mizuno, I. Nakayama, N. Aoi, M. Kubota, and T. Komeda, *Appl. Phys. Lett.*, **53**, 2059 (1988).
11. C. Yu and N. W. Cheung, *IEEE Electron Device Lett.*, **EDL-15**, 196 (1994).
12. J. Nishizawa, K. Aoki, and T. Akamine, *Appl. Phys. Lett.*, **56**, 1334 (1990).
13. S. Matsumoto, S. Yoshioka, J. Wada, S. Imai, and K. Uwasawa, *J. Appl. Phys.*, **67**, 7204 (1990).
14. X. Y. Qian, N. W. Cheung, and M. A. Lieberman, *Appl. Phys. Lett.*, **59**, 348 (1991).
15. T. Inada, A. Kuranouchi, H. Hirano, T. Nakamura, Y. Kiyota, and Y. Onai, *ibid.*, **58**, 1748 (1991).
16. T. Hara, S. Nakagawa, K. Shinada, and S. Nakamura, *ibid.*, **63**, 90 (1993).
17. T. Hara, K. Shinada, and S. Nakamura, *Jpn J. Appl. Phys.*, **33**, 5608 (1994).
18. A. Hasegawa, R. I. Kang, and K. Shono, *Trans. IEICE Jpn.*, **J75-C-II**, 28 (1992).
19. A. Hasegawa, R. I. Kang, and K. Shono, in *Proceedings of 1992 IEEE International Conference on Semiconductor Electronics*, Malaysia, p. 213, IEEE (1992).
20. F. M. Smits, *BSTJ*, **36**, 711 (1958).
21. B. Mcdonald and A. Goetsberger, *This Journal*, **109**, 141 (1962).
22. S. D. Rosenbaum, *Solid-State Electron.*, **11**, 711 (1968).
23. J. C. Irvin, *BSTJ*, **41**, 387 (1962).
24. C. T. Sah and H. C. Pao, *IEEE Trans. Electron Devices*, **ED-13**, 393 (1966).
25. W. Kern and D. A. Puotinen, *RCA Rev.*, **31**, 187 (1970).
26. Y.-C. Tseng and K. Shono, *Jpn. J. Appl. Phys.*, **28**, L329 (1989).
27. Y.-C. Tseng and K. Shono, *ibid.*, **30**, L222 (1991).
28. O. Kudoh, K. Nakamura, and M. Kamoshida, *J. Appl. Phys.*, **45**, 4514 (1974).
29. J. R. Brews, *IEEE Trans. Electron Devices*, **ED-26**, 1696 (1979).

Modeling of the Wear Mechanism during Chemical-Mechanical Polishing

Chi-Wen Liu,[a] Bau-Tong Dai,[b] Wei-Tsu Tseng,[b] and Ching-Fa Yeh[a]

[a]*Department of Electronics Engineering and Institute of Electronics, National Chiao Tung University, Hsinchu, Taiwan*
[b]*National Nano Device Laboratory, Hsinchu, Taiwan*

ABSTRACT

A model based on statistical method and elastic theory is presented to describe the wear mechanism of the silicon wafer surface during chemical-mechanical polishing. This model concerns the effects of applied pressure and relative velocity between the pad and the wafer on the removal rate during polishing and is capable of delineating the role of the mechanical properties of the slurry particles and the films to be polished. The removal rate is dependent on the elastic moduli of slurry particle and polished film. Comparisons with experimental data demonstrate the validity of the model for predicting relative removal rate for various dielectric films.

Introduction

The increasing complexity of device designs and the emergence of deep submicrometer structures require minimum surface topographies for future lithography requirements in the integrated circuit (IC) industry. Surface topographies are reduced using advanced planarization processes like thermal flow, bias-sputtered dielectrics, etchback, and spin-on glass.[1-3] However, it is generally agreed that conventional techniques merely smooth the topography locally and have no significant effect on global planarization. A new planarization method, called chemical-mechanical polishing (CMP), has become widely accepted for planarizing interlevel dielectrics[4,5] and for selective removal of aluminum,[6] tungsten,[6,7] copper,[8] and titanium[9] overburden following metal filling of studs and interconnects.

CMP involves simultaneous and intimate contact between the wafer surface and a pad charged with a layer of colloidal silica slurry. The relative motion between the wafer and pad, combined with applied pressure and chemical activity of the slurry results in abrasion of the wafer surface. Specifically, when a particle embedded in the fibers of the pad has sufficient strength and energy to overcome the fracture toughness of polished material, strikes the wafer surface, material is removed from the surface. Unfortunately, it is difficult to design experiments to separate out the effects of a particular consumable from other controlled variables that affect the removal rate, such as the type of pad, film properties, slurry characterization, and pad conditioning. Hence, not many details about CMP removal mechanisms are available. This lack of understanding of polishing mechanics and chemistry sets limits on the ability of experimentally based statistical methods to improve the process, and is a major drawback to adopting CMP for manufacturing. Consequently, a wear model is urgently needed to upgrade understanding of CMP removal mechanisms, and to relate process parameters to actual material removal.

To better understand the polishing physics from various science and engineering fields, wafer-scale and feature-scale physics have been modeled by various researchers. The most common wafer-scale model for material removal is Preston's equation,[10] where removal rate of material is

Downloaded on 2014-04-28 to IP 140.113.38.11 address. Redistribution subject to ECS terms of use (see ecsdl.org/site/terms_use) unless CC License in place (see abstract).

related to the work per unit time done on each unit area of the surface to be polished. Cook[11] reviewed the mechanics and chemical polish of glass polishing, which has significant association with CMP of silicon dioxide. In his analysis, a microcutting mechanism was proposed to simulate the breaking of chemical bonds which result from interaction of both the glass surface and polishing particle with water. From the field of tribology, Runnels and Eyman[12] analyzed the behavior of the fluid film between the wafer and the pad. Hydrodynamic lubrication is, however, only responsible for distributing the slurry, and microcutting of polished film due to solid-solid contact has not been used to characterize the process.

Burke[5] introduced a semiempirical model of SiO_2 polishing, and gave insights into the effects of "down" area dimensions, "up" area patterning, and feature step height. Warnock[13] presented a phenomenological model that describes the CMP process. This model, which intuitively assumes partial wafer-pad contact, can predict erosion profile of array of features with different sizes and pattern density. Runnels[14] proposed a feature-scale model for polishing using a hydrodynamic slurry layer that bridges the gap between wafer- and particle-scale models through layer-thickness and erosion laws. Another modeling approach[15] assumed that material removal is related to "sharp edges," which are defined as slurry particles embedded in the fibers of the polishing pad that have sufficient force to increase their effective masses to the point where polishing can occur. Thus, distribution of effective sharp edges determines the removal rate and uniformity of polished surface. All the above models, however, have not proven satisfactory enough at distinguishing among consumables which affect removal rates. There is still a need to develop models for fundamental understanding of the process that can be used as a base for process development.

In the CMP process the real contact area between slurry particles and the wafer surface, that dominates the removal of material from the wafer surface, is different for various combinations of dielectric films and slurry particles due to their differing surface mechanical properties. Therefore, knowledge of the contact area, wafer surface mechanical properties, and slurry particle characteristics is critical in determining the removal-rate predictions. So far, little has been reported on this subject. For this reason, wear analysis was performed to enhance our understanding of wafer-surface/slurry-particle contact mechanics during the CMP process. Our previous work[16] reported a linear relationship between removal rate and film hardness. Cook's review[11] proposed a 1/modulus-dependence removal rate. Therefore, one may intuitively correlate the removal rate with a "mechanical factor" of hardness/modulus as we pointed out previously.[16] We describe here a more complete erosion model based on statistical mechanism and elastic theory which fits removal rates for dielectric films. This allows quantitative evaluation of a given CMP process and provides a basis for process optimization to meet specific technological requirements, such as selective polishing processes.

Experimental

Preparation of dielectric films.—All test samples were prepared on p-type (100), 150 mm silicon wafers. Thermally grown silicon dioxide films were obtained by wet oxidation (ASM/LB45 furnace system), in which the silicon was exposed to an ambient of H_2 and O_2 at 980°C. Films of plasma-enhanced chemical-vapor deposition (PECVD) oxide were deposited with the AMT/P5000 system, tetraethylorthosilicate (TEOS) and O_2 at 390°C were used as a reactant gas for TEOS-PECVD films; SiH_4, N_2, and NH_3 at 400°C for deposition of Si_3N_4-PECVD films. Silicon-rich oxide (SRO-PECVD) films were obtained in ambient SiH_4, N_2, and N_2O at 400°C with a Novellus reactor. All specimens were deposited to a thickness of $\sim$1 μm.

Polisher setup.—A Westech Model 372M CMP processor, consisting of an IC 1000/Suba IV (made of polyurethane impregnated polyester) pad affixed to a circular polishing table and a carrier to hold wafers against the pad, was used for polishing. During the polish experiment, the wafer was mounted on a template assembly for a single 6 in. diam wafer. The Teflon retaining ring is recessed from the wafer surface by 7 mil. Pressure at the wafer-slurry-pad interface is controlled via an overhead mechanism which allows pressure to be applied to the wafer holder. Both the carrier and table were rotated independently. The thickness of the dielectric film was measured with Nanometrics 2100XP by a 10 mm edge exclusion, and was averaged over nine different locations on the wafer to determine the polish rate. Cross-wafer nonuniformity of the dielectric polish rate was less than 10%. The polish slurry (SC-1 slurry available from Rippey Corp.) was a suspension of fumed silica dispersed in aqueous potassium hydroxide. To allow for removal-rate variations from run to run, the removal rate ratio (*R. R. ratio*) is defined as

$$R.R.\ ratio = \frac{\text{Removal rate of dielectric film}}{\text{Removal rate of thermal oxide}}$$

Pad conditioning.—Pad conditioning techniques were used to refurbish the pad surface to maintain the removal rate without sacrificing uniformity. In our experiments, pad conditioning with Rotating Pad Conditioner II was performed between each wafer to clean the slurry residue and to lift the pad fibers for further processing. Without this procedure, the polish rate decreased substantially after only several wafers. Our polish experiments were carried out under well-controlled conditions, as described in our previous study,[16] *e.g.*, pad conditioning was performed before and between each wafer, and polishing was terminated before pad glazing could cause significant decrease in removal rate.

Nanoindentation measurement.—Young's modulus data were determined using the NanoTest 500 mechanical properties microprobe developed at Micro Materials Ltd. (UK). Nanoindentation loads are applied through a coil and magnet assembly. The position of the indenter is measured by capacitive sensors. The indenter probe is a three-sided pyramid (Berkovich) which projects an equilateral triangle on the sample. Theoretically, the area can be calculated if the displacement is known. At very shallow depths, the tip of the indenter is not perfect, so the depth-to-area relationship was calibrated with fused silica,[17,18] since it has a very smooth surface and isotropic elastic properties. Thus precise reproducible data can be obtained at shallow depths without having to image the indent. Here, the loading rate was set at 1.18 mN/s to a maximum depth of 300 nm and the ambient temperature was held at 22.7°C. We assumed that the substrate did not significantly affect the modulus value obtained by indenting into the first 300 nm of the 1 μm thick films. For each sample, ten separate indents, spaced 15 μm from each other, were made on the surface under investigation.

Modeling

To begin with, we consider the process of rolling as an analogy to the CMP removal mechanism in which wafers are being pressed down against the pad, and slurry particles are moving in the gap between the wafer and the pad in a shearing (cutting) action. Kragelsky *et al.*[19] proposed the kinematics of an abrasive particle moving in the gap of a rolling-contact pair. From statistical mechanism, they assumed (*i*) the velocity ν of the abrasive particle is a linear combination of the velocities of the two surfaces ν_1 and ν_2, respectively, *i.e.*

$$\nu = \alpha\nu_1 + \beta\nu_2 \quad [1]$$

where α and β are the probability of adherence of the particles to surface 1 and surface 2, respectively, mean values of which can be assumed to be approximately inversely proportional to the Brinell hardness values of surface $1(HB_1)$ and surface $2(HB_2)$, *i.e.*

Downloaded on 2014-04-28 to IP 140.113.38.11 address. Redistribution subject to ECS terms of use (see ecsdl.org/site/terms_use) unless CC License in place (see abstract).

$$\alpha = \frac{HB_2}{HB_1 + HB_2} \quad [2]$$

$$\beta = \frac{HB_1}{HB_1 + HB_2} \quad [3]$$

$$\alpha + \beta = 1 \quad [4]$$

(*ii*) A spherical model of a particle of diameter $2R$ under uniform load F penetrates the two mated surfaces. The depth of penetration of the particle into the two mated surfaces depends on the surface hardness of the particle and of the two mated surfaces. (*iii*) Abrasive particles do not rupture in the load-contact range until the maximum depth of penetration into the surface materials corresponds to rupture strength of the particles.

From the above simplification, the time t of contact of abrasive particle in the gap between the mated surfaces from the point of its introduction into the gap to the point, where it attains a depth of penetration (h_1 for surface 1 and h_2 for surface 2), can be given by[19]

$$t = \sqrt{\frac{\rho^*}{R}}\left[\frac{(HB_1 + HB_2)\,h_1}{HB_2\,(\alpha\nu_1 + \beta\nu_2)}\right] \quad \text{(for surface 1)}$$

$$= \sqrt{\frac{\rho^*}{R}}\left[\frac{(HB_1 + HB_2)\,h_2}{HB_1\,(\alpha\nu_1 + \beta\nu_2)}\right] \quad \text{(for surface 2)} \quad [5]$$

where

$$\rho^* = \frac{\rho_1\,\rho_2}{\rho_1 + \rho_2} \quad [6]$$

ρ_1 and ρ_2 are the radii of curvature of surface 1 and surface 2, respectively.

During the interval of time t, the abrasive particle moves in the gap between the mated surfaces with ever-increasing penetration into the contact materials and deforms a certain volume G of the surface material. The deformed volume can be expressed as[19]

$$G = \frac{\sqrt{2\rho^*}}{3}(h_1)^{5/2}\left[\frac{HB_1}{(\alpha\nu_1 + \beta\nu_2)\,HB_2}\right]V \quad \text{(for surface 1)}$$

$$= \frac{\sqrt{2\rho^*}}{3}(h_2)^{5/2}\left[\frac{HB_2}{(\alpha\nu_1 + \beta\nu_2)\,HB_1}\right]V \quad \text{(for surface 2)} \quad [7]$$

where $V = |\nu_1 - \nu_2|$ is the relative velocity between surface 1 and surface 2.

CMP is a method of planarization where the wafer is pressed facedown by a carrier and rotated against a polishing pad covered with a layer of slurry. The pad is used to hold the slurry particles, transmit load forces to the particle/wafer surface, and conform precisely to the film being polished. A schematic representation of the settling of the slurry particle into the gap between the surface of the wafer and the pad is illustrated in Fig. 1. Since the role of hydrodynamic lubrication of the fluid film is distributing the slurry,[12] lowering friction force, and removing abraded chips and heat generated by the CMP process, the slurry particles are in direct contact with both the pad and the surface of the wafer during the polishing process. Since hardness is a determining factor in how deeply a particle (slurry-carried particles in the case of CMP) penetrates into a surface, the harder the deformed material, the less it is penetrated under a given load. Thus, the depth of penetration into the pad surface (made of polyurethane which is softer) was assumed to be greater than into the surface of the wafer as schematically shown in Fig. 1.

During CMP, the slurry particles move between the wafer and the pad. Figure 2 is a schematic representation of the slurry-particle/wafer-surface system in which slurry particle moves along the wafer surface from engagement point (point c) into the wafer to the depth of penetration $\overline{od}$. Local pressure at the point of contact in the system is at times largely determined by the nature of the polishing lap. Thus, the microvolumes G_{abcd} on the contact surfaces as shown in Fig. 3 undergo elastic and plastic deformation or microcutting depending on the depth of penetration. The conditions for these deformations are determined by certain transition criteria,[19] *i.e.*, h_{ep}, the criterion for transition from elastic to plastic deformation and h_{pm}, the criterion for the transition from plastic deformation to microcutting. By means of these criteria, the deformed volumes can be separated into three regions (Fig. 3), *e.g.*, regions of elastic deformation G^e, plastic deformation G^p, and microcutting G^m.

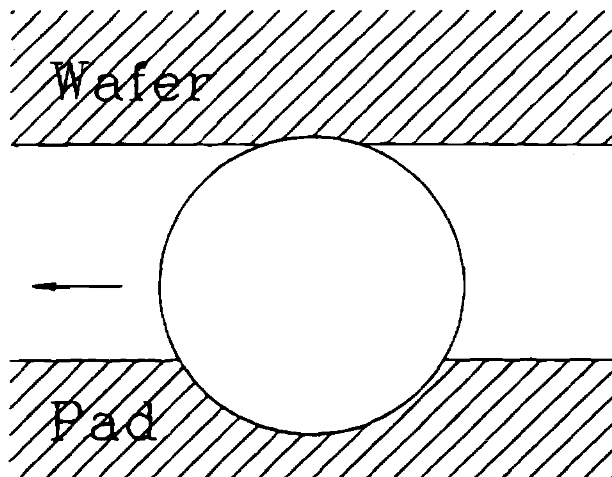

Fig. 1. Schematic representation for the settling of the slurry particle into the gap between the surface of the wafer and the pad.

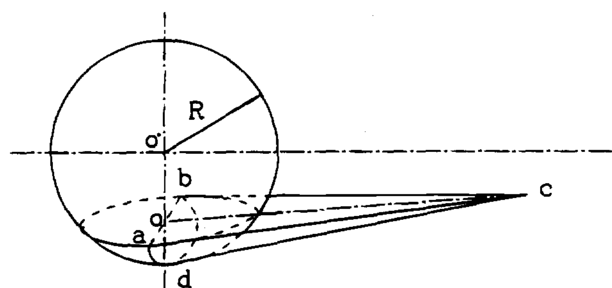

Fig. 2. Schematic representation of the contact between slurry particle (of radius R) and wafer surface performed by moving the slurry particle on the wafer surface from the engagement point (point c) to a depth of penetration $\overline{od}$ into the wafer.

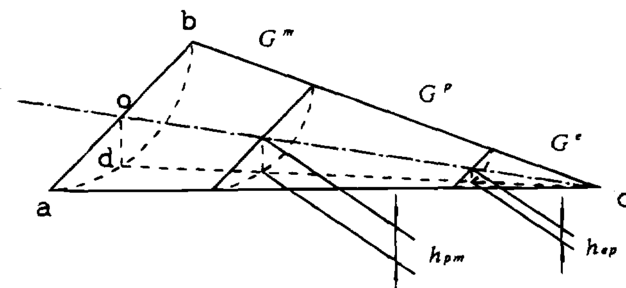

Fig. 3. Regions of elastic deformation G^e, plastic deformations G^p, and microcutting G^m from the introduction point (point c) of slurry particle to a depth of penetration $\overline{od}$.

Downloaded on 2014-04-28 to IP 140.113.38.11 address. Redistribution subject to ECS terms of use (see ecsdl.org/site/terms_use) unless CC License in place (see abstract).

Generally, ceramic materials such as SiO_2 and Si_3N_4 have an insufficient number of independent slip systems by which general deformation can occur and may have structures that are so complex dislocation motion is difficult.[20] Thus, on loading the surface of a dielectric by an indenting particle, deformation is directly transformed from elastic deformation to microcutting with little or no intermediate transitional time. Only a limited amount of plastic deformation is possible in this process. Also, since the elastic deformation occurs at low load levels, the deformation volume is small compared with the volume of microcutting due to overloading. We assumed therefore the deformation volume during contact time to be approximately equal to the volume of microcutting, *i.e.*

$$G_{abcd} = G^m >> G^e + G^p \quad [8]$$

Dividing the deformed volume G_{abcd} by the contact time t, the removal rate ($R. R.$) can thus be obtained

$$\begin{aligned} R.R. &= \frac{G_{abcd}}{t} \\ &= \left(\frac{\sqrt{2}}{3}\right) h_2^{1.5} R^{0.5} V \left(\frac{HV_2}{HV_1 + HV_2}\right) \\ &= \left(\frac{\sqrt{2}}{3}\right) h^{1.5} R^{0.5} V \left(\frac{HV_w}{HV_p + HV_w}\right) \\ &= \frac{\sqrt{2R}}{3} (h)^{3/2} V \left(\frac{HV_w}{HV_p + HV_w}\right) \end{aligned} \quad [9]$$

where the Vickers' hardness numbers (HV) are used for thin films and the surfaces of the wafer and of the pad correspond to surface 2 and surface 1, respectively; *e.g.*

$$h_2 = h \quad HV_2 = HV_w \quad HV_1 = HV_p \quad [10]$$

The real contact area A_k as assumed by Kragelsky *et al.*[19] can be expressed in terms of radius R and depth of penetration $\overline{od} = h$ of the slurry particle, hence

$$A_k = 2\pi Rh \quad [11]$$

The problem now becomes how to determine the depth of penetration h. Let us consider a case in which two elastic bodies, say, two balls, are pressed against each other by external forces. The pressure is distributed over a small circle of contact formed as a result of local deformation. The radius r of the contact circle is given by the elasticity equation proposed by Hertz[21]

$$r = 0.88\left[\frac{F(E_2 + E_3)d_2d_3}{2E_2E_3(d_2 + d_3)}\right]^{\frac{1}{3}} \quad [12]$$

where E_2 and E_3 are the moduli of the two balls and d_2 and d_3 the corresponding radius; F is applied force.

Similarly, a slurry particle penetrates a flat dielectric plane with R_f radius of curvature due to force applied to the slurry-particle/wafer-surface system (Fig. 4). Hence, the radius r of the contact circle derived from the Hertzian theory can be approximated by

$$r = 0.88\left[\frac{F(E_s + E_w)RR_f}{2E_sE_w(R + R_f)}\right]^{\frac{1}{3}} \quad [13]$$

where the surface of the wafer and the slurry particle are equal to ball 2 and ball 3, respectively, namely

$$E_2 = E_w \quad E_3 = E_s \quad d_2 = R_f \quad d_3 = R \quad [14]$$

Assuming the wafer surface to be a plane surface, R_f is thus very large and $R << R_f$, Eq. 13 can be simplified to

$$r = 0.88\left[\frac{F(E_s + E_w)R}{2E_sE_w)}\right]^{\frac{1}{3}} \quad [15]$$

Thus, the real contact area A_H from Hertz's theory can be expressed as

$$\begin{aligned} A_H &= \pi r^2 \\ &= \pi\left(0.88\left[\frac{F(E_s + E_w)R}{2E_sE_w}\right]^{\frac{1}{3}}\right)^2 \end{aligned} \quad [16]$$

The real contact area, calculated either according to Kragelsky *et al.*[19] or to Hertz,[21] should be equal, *i.e.*

$$A_k = A_H \quad [17]$$

Thus,

$$2\pi Rh = \pi\left\{0.88\left(\frac{F(E_s + E_w)R}{2E_sE_w}\right)^{\frac{1}{3}}\right\}^2 \quad [18]$$

Depth of penetration h is thus calculated as

$$h = C\left[\left(\frac{E_s + E_w}{E_sE_w}\right)\frac{F}{\sqrt{R}}\right]^{\frac{2}{3}} \quad [19]$$

where C is a constant. Substituting Eq. 19 into Eq. 9

$$\begin{aligned} R.R. &= CA\left(\frac{HV_w}{HV_w + HV_p}\right)\left(\frac{E_s + E_w}{E_sE_w}\right)\left(\frac{F}{A}\right)V \\ &= C'\left(\frac{HV_w}{HV_w + HV_p}\right)\left(\frac{E_s + E_w}{E_sE_w}\right)PV \end{aligned} \quad [20]$$

where A is the area of the wafer. C' also contains the chemical effect which is perceived as being independent from mechanical factors and is constant assuming fixed slurry chemistry. Equation 20 indicates that surface mechanical properties of the wafer, the pad, and the slurry particle, such as hardness and Young's modulus, play significant roles in the polishing rate. When other controlled variables are fixed, Eq. 20 predicts that removal rate will decrease with increasing pad hardness, which is in agreement with previous reports.[15]

Generally, the wafer surface is hard and brittle, while the pad, typically polyurethane-based materials, is much softer, *i.e.*, $HV_p << HV_w$. Hence removal rate can be simplified to

$$\begin{aligned} R.R. &= C''\left(\frac{E_s + E_w}{E_sE_w}\right)PV \\ &= C''\left(\frac{1}{E_s} + \frac{1}{E_w}\right)PV \end{aligned} \quad [21]$$

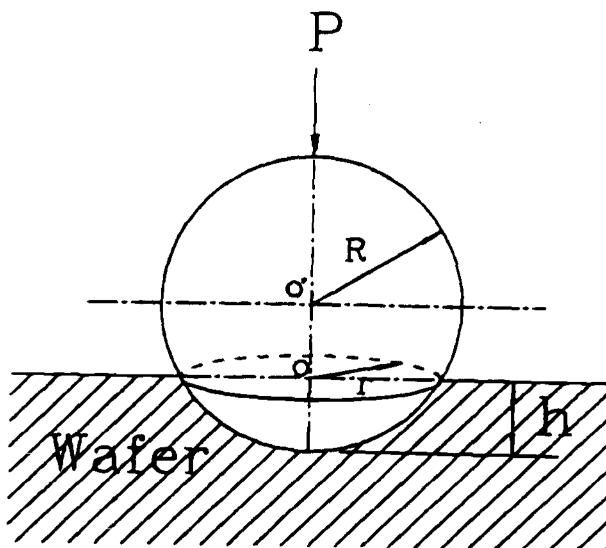

Fig. 4. Mechanics of slurry particle/wafer surface contact.

Downloaded on 2014-04-28 to IP 140.113.38.11 address. Redistribution subject to ECS terms of use (see ecsdl.org/site/terms_use) unless CC License in place (see abstract).

While Eq. 21 excludes the effect of HV_p on the removal rate, we do not, however, rule out the significance of pad characteristics in polishing behavior. In real cases, removal rate is very slow when smooth pads are used because the slurry particles cannot be held in the fibers of the pad.[15] The influence of the surface morphology of the pad on polish rate and uniformity is still an area that requires further investigation and is outside our present scope.

A wear model for the CMP process similar in form to Preston's equation has been developed and has the particularity of separating out the mechanical properties of the slurry particle and the surface of the wafer from Preston's coefficient. To summarize, the kinetics of polishing are: *(i)* the rate of material removal is dependent on the real contact area between the slurry particle and the surface of the wafer. The real contact area is determined by applied pressure, the curvature, and Young's modulus of the slurry particle and the surface of the wafer; *(ii)* the removal rate increases linearly with increasing applied pressure and relative velocity between the pad and the surface of the wafer, as in Preston's equation; and *(iii)* the removal rate increases as a result of a reduction in the modulus of slurry particle or film to be polished.

The model we developed herein relates removal rate to measurable material properties and hence provides a simple and explicit way to monitor the CMP process. Experimental results with various dielectric films are presented and discussed in the next section.

Results and Discussion

Effect of pressure and rotation velocity on the removal rate of dielectric film.—Our wear model, similar to Preston's equation, suggests that material removal is directly proportional to the applied pressure and relative rotation speed. We investigated the characteristics of the CMP process and observed that an increase in polish pressure and pad rotation speed promoted the removal rate,[4] while carrier rotation speed, back pressure, and increased slurry flow have a less pronounced effect on the polishing rate. We also found that adjustments in the pad and carrier speed determine the polishing uniformity, and that increased back pressure leads to more uniform removal. Details about the effects of polish pressure and rotation speed on removal rate can be found in our previous report.[4]

Effect of the modulus of the dielectric film on experimental erosion data.—To examine the role of the modulus of the dielectric film on polish rate, four kinds of dielectric film including Si_3N_4-PECVD film, thermal oxide, SRO-PECVD, and TEOS-PECVD film were used. Young's moduli of various dielectric films were obtained from nanoindentation measurements and are listed in Table I. It was clearly observed that the value of Young's modulus of the Si_3N_4 film, 221 GPa, was much larger than those of oxide films. This is because the basic structure of Si_3N_4 consists of an SiN_4 tetrahedron shared by three other SiN_4 tetrahedra to form a three-dimensional network. The Si-N bond is formed by the overlapping of the sp^3 orbital of the silicon and the sp^2 orbital of the nitrogen with additional π-bonding from the nitrogen to the empty 3d level of the silicon. This creates an exceptionally strong bond in Si_3N_4, producing a rigid structure with a Young's modulus greater than three times that of quartz. The oxygen atoms in the SiO_2 form a silicate network sharing only two tetrahedra.[22] Further, the value of modulus of the oxide film is notably dependent on the type of precursor used and on deposition technique. This suggests that variations in modulus of oxide films is the result of hydrogen incorporation, the presence of defects, microvoids, clusters, and dangling bonds due to various preparation processes. The measured values of modulus of thermal oxide, SRO-PECVD, and TEOS-PECVD are 73, 70.9, and 69 GPa, respectively, which are consistent with recent studies.[22,23]

As Eq. 21 predicts, removal rate is affected by the combination of moduli of slurry particle and polished film when other process variables are fixed. We proceeded to examine two real cases involving dielectric polish processing

Oxide films polished with silica particles.—Since the PECVD oxide films and silica particles were prepared by vapor deposition methods and have virtually the same SiO_2 network structure, it can be assumed that no difference exists between the moduli of these oxides. Thus, by substituting $E_s = E_w$ into Eq. 21, the removal rate becomes

$$R.R. = C''\left(\frac{2}{E_w}\right)PV \qquad [22]$$

Equation 22 indicates that removal rate is inversely proportional to modulus of polished films, same as the erosion model in Cook's review. Experimental data show good agreement with predicted results when compared with the removal rate and modulus for thermal oxide, SRO-PECVD, and TEOS-PECVD films as shown in Table I.

Si_3N_4 films polished with silica particles.—Cook's model implies inherently equal modulus for polished films and slurry particles so that the difference in mechanical properties between the "polisher" and the "polished" is ignored and its role in removal rate is underestimated. Since the modulus of Si_3N_4 is much larger than that of silica, the relationship between removal rate and modulus of polished film thus should not follow Cook's model, and a large deviation was observed as shown in Table I. Removal rate data based on our model show a close match with the experimental values.

As discussed above, our model presents a more general expression of removal rate (Eq. 20) which includes both hardness and modulus of the materials involved in the polishing action. This model does predict the same removal rate PV dependence as in Preston's equation and can be extended to cases where slurry and film properties are discernible. For slurry and film with the same modulus, our model reduces to a special case of Cook's model as in Eq. 22. For slurry and film of differing mechanical natures, Eq. 21 weighs the contributions of the two moduli and yields a better prediction of removal rate. Although our polish experiments were all carried out under most stable conditions as described earlier, as much as a 15% mismatch still exists between our modeled data and the experimental data. This can be attributed to inhomogeneity of film properties, uneven slurry distribution, temperature variations, and other transient variables.

For CMP of metal films, the desirable processes are first the formation of an insoluble and hard passivation layer on the metal surface through chemical reactions with slurry and then removal of the passivation layer by mechanical polishing or simply "rubbing," leaving a fresh metal surface for continuing chemical reaction, and then repeating the process.[6,7] In light of this proposed scenario, the removal rate may not be governed merely by mechanical actions, the chemical reaction rate may play a more significant role in the removal mechanism. In addition, the large volume of plastic deformation of metals necessitates the inclusion of the G^p term in Eq. 8, which complicates

Table I. Comparison of removal rate ratio (R. R. ratio) from experimental results, predicted data from Cook,[11] and from our wear model.

Dielectric	Young's modulus (GPa)	*R. R. ratio* (Experimental)	*R. R. ratio* (from Cook's)	*R. R. ratio* (from our model)
Si_3N_4-PECVD	221	0.59	0.33	0.68
Thermal oxide	73	1	1	1
SRO-PECVD	70.9	1.08	1.03	1.01
TEOS-PECVD	69	1.22	1.06	1.04

Downloaded on 2014-04-28 to IP 140.113.38.11 address. Redistribution subject to ECS terms of use (see ecsdl.org/site/terms_use) unless CC License in place (see abstract).

the modeling process. In short, extension of the proposed wear model to metal CMP requires major revision and is currently under investigation by our team.

Conclusion

An *ab initio* wear model for CMP processing has been developed based on kinematics and elastic theory. The model described herein has been demonstrated to possess the ability to link process variables including applied pressure and relative rotation speed between the polishing pad and the wafer being polished to removal rate, and has the particularity of correlating the effects of mechanical properties of the slurry particles and polished film with removal rate through approximation of the contact area. Increases in polishing pressure and pad speed have been shown to promote the polish rate as predicted by our model. However, it must be emphasized that pad glazing and inadequate pad conditioning result in degradation of removal rates due to poor slurry transport. Elastic moduli of slurry and the dielectric to be polished are shown to be critical factors in determining the CMP removal rates. Preliminary experimental results indicate that for slurry and dielectric with the same modulus (*e.g.*, SiO_2 polished by silica), the current model reduces to a special case of Cook's model in which removal rate is inversely proportional to the film modulus. For dielectric and slurry with differing mechanical properties (*e.g.*, Si_3N_4 polished by silica), our model is able to sort out the effects of the two contributing moduli and give a more faithful prediction of removal rates. Thus, the type of wear mechanism demonstrated has the potential of not only increasing understanding of, but also optimizing the polishing process.

Acknowledgment

The authors express appreciation for helpful discussions with Dr. T. Y. Yen in the Institute of Mechanical Engineering, National Chiao Tung University. This work is supported by UMC, TSMC, and National Science Council (NSC84-2622-E009-007), R.O.C. The Young's modulus measurements were made possible by the assistance of the Precision Instrument Development Center in providing the NANOTEST 500 used for these experiments.

Manuscript submitted May 16, 1995; revised manuscript received Sept. 25, 1995.

National Nano Device Laboratory assisted in meeting the publication costs of this article.

REFERENCES

1. S. Sivaram, H. Bath, R. Leggett, A. Maury, K. Monnig, and R. Tolles, *Solid State Technol.*, **35**, 87 (1992).
2. I. Ali, S. R. Roy, and G. Shinn, *ibid.*, **37**, 63 (1994).
3. P. H. Singer, *Semicond. Int.*, **15**, 44 (1992).
4. B. T. Dai, C. W. Liu, and C. F. Yeh, in *Proceedings of the First International Dielectrics for VLSI/ULSI Multilevel Interconnection Conference (DUMIC)*, p. 149 Santa Clara, CA (1995).
5. P. A. Burke, in *Proceedings of the 1991 VLSI Multilevel Interconnect Conference (VMIC)*, p. 379, New York (1991).
6. C. Yu, A. Laulusa, M. Grief, and T. T. Doan, in *Proceedings of the 1992 VLSI Multilevel Interconnect Conference (VMIC)*, p. 156 (1992).
7. F. B. Kaufman, D. B. Thompson, R. E. Broadie, M. A. Jaso, W. L. Guthrie, D. J. Pearson, and M. B. Small, *This Journal*, **138**, 3460 (1991).
8. J. M. Steigerwald, R. Zirpoli, S. P. Murarka, D. Price, and R. J. Gutmann, *ibid.*, **141**, 2842 (1994).
9. J. M. Steigerwald, S. P. Murarka, R. J. Gutmann, and D. J. Duquette, *ibid.*, **141**, 3512 (1994).
10. F. Preston, *J. Soc. Glass Technol.*, 11 (1927).
11. L. M. Cook, *J. Non-Crystal. Solids*, **120**, 152 (1990).
12. S. R. Runnels and L. M. Eyman, *This Journal*, **141**, 1698 (1994).
13. J. Warnock, *ibid.*, **138**, 2398 (1991).
14. S. R. Runnels, *ibid.*, **141**, 1900 (1994).
15. H. T. Sanford-Crane, Westech System Incorporated, Phoenix, AZ.
16. C.-W. Liu, B.-T. Dai, and C.-F. Yeh, *This Journal*, **142**, 3098 (1995).
17. M. F. Doerner and W. D. Nix, *J. Mater. Res.*, **1**, 601 (1986).
18. W. C. Oliver and G. M. Pharr, *ibid.*, **7**, 1564 (1992).
19. I. V. Kragelsky, M. N. Dobychin, and V. S. Kombalov, *Friction and Wear, Calculation Methods,* Chap. 11, pp. 352-366, Pergamon Press, Ltd., New York (1982).
20. W. Hayden, W. G. Moffatt, and J. Wulff, in *Structure and Properties of Materials*, J. Wulff, Editor, Vol. 3, Chap. 9, pp. 189-217, John Wiley & Sons, Inc., New York (1971).
21. S. Timoshenko, *Strength of Materials*, pp. 339-345, D. Van Nostrand Co., Inc., Princeton, NJ (1982).
22. J. A. Taylor, *J. Vac. Sci. Technol.*, **A9**, 2464 (1991).
23. J. M. Grow and R. A. Levy, *J. Mater. Res.*, **9**, 2072 (1994).

Downloaded on 2014-04-28 to IP 140.113.38.11 address. Redistribution subject to ECS terms of use (see ecsdl.org/site/terms_use) unless CC License in place (see abstract).